

# OPTIMIZATION OF BEAM DYNAMICS FOR AN S-BAND ULTRA-HIGH GRADIENT PHOTOINJECTOR\*

A. Cahill<sup>†</sup>, A. Fukasawa, J. Rosenzweig, UCLA, Los Angeles, CA, USA  
C. Limborg, Weilun Qin, SLAC, Menlo Park, CA, USA

## Abstract

New electron sources with improved brightness are desired to enhance the capabilities of FELs, making them more compact and fully coherent. Improvements in electron source brightness can be achieved by increasing electric fields on the cathode of photo-emitted electron guns. Recent developments in pulsed RF accelerator structures show that very high gradient fields can be sustained with low breakdown rates by operating at cryo-temperatures, which when applied to photoguns will lead to a large increase in the electron beam brightness. In particular, our simulations show that when operating with a peak gradient field of 240 MV/m on the cathode of an S-band, electron beam brightness of  $80 \text{ nC}/(\text{mm} \cdot \text{mrad})^2/\text{mm}$  can be achieved with 100 pC bunches. In this paper, we present the design and optimization of an 1.x cell S-Band RF photoinjector, where the x varies from 4-6. The optimization in brightness has been obtained by using a multi-objective genetic algorithm on the solutions calculated with the ASTRA code. We calculate the optimum length of the rf gun, position of accelerating structure, and laser pulse dimensions for a variety of charges.

## INTRODUCTION

The introduction of the BNL/UCLA/SLAC style rf photoinjectors 25 years ago led to an increase in the peak brightness of electron sources [1]. Notably, this enabled the Linac Coherent Light Source (LCLS), a free electron laser (FEL) located at SLAC, to attain first light and FEL saturation in 2009 [2]. This was possible using a 2.856 GHz 1.6 cell radio frequency (rf) photoinjector. The rf gun had been designed to operate at 140 MV/m and to run 1 nC, but has been operated at 120 MV/m for typically 150 pC and 20 pC [3]. It is possible to improve present performance of the LCLS injector by modifying the laser pulse shaping and changing the booster linac position [4].

Ultra-Fast Electron Diffraction (UED) instruments using MeV electron beams have also benefited from the development of electron sources for FELs. They now promise to become competitive with FELs for a variety of experiments once the anticipated improvements in the electron sources are demonstrated [5].

A collaboration between UCLA, SLAC, and INFN is working on improving the peak brightness of electron sources by increasing the maximum operating gradient

on the photocathode. Experimental results obtained at SLAC have demonstrated that surface electric fields of near 500 MV/m can be achieved at 11.4 GHz with low breakdown rates by operating normal conducting accelerating structures at cryogenic temperatures near 45 K, against 375 MV/m at normal temperature[6]. This collaboration proposes to apply this idea to a S-band rf photoinjector with cathode operating electric field gradients of 240 MV/m. Calculations based on the results achieved at X-Band show that cathode gradient fields of 240 MV/m will be possible at S-Band, with low breakdown rates and manageable dark current. The increase in the current electron source brightness will lead to better FEL performance, both shorter gain lengths, and higher energy X-rays [5].

To explore the possibilities of a ultra-high gradient rf photoinjector we have used a multi-objective genetic optimizer as developed at LBNL[7, 8]. This optimizer uses the NSGA-II genetic algorithm[9, 10]. The two objectives of the optimization are a small transverse emittance and a small bunch length. Pareto improvements were explored to maximize the peak brightness. Depending on the application, the maximum peak brightness might not be the best solution. For instance, in an FEL where compression is implemented downstream of the injector, a minimum emittance might be better to maximize the energy output of the FEL pulse. Full start-to-end simulations including possible degradation of the emittance are needed for deciding what is the best compromise between emittance and bunch length in the injector. For a UED electron source, very short bunch length can be the primary goal.

## METHODS

### *Electric Field Maps*

The electric field maps for the rf gun were generated in SUPERFISH[11], for the 1.4, 1.45, 1.5, 1.55, and 1.6 cell geometries, What is referred to as a cell in an rf gun is the length of  $\lambda/2$ . Therefore, a 0.6 length cathode cell will have length  $0.3 * \lambda$ , and a 1.6 cell gun would have a total length of  $0.8 * \lambda$ . The frequency was tuned to 2.856 GHz and with the electric field balanced between the partial cell where the electrons are launched and the full cell. The procedure and geometry for this specific style of rf photoinjector is fully explained in [12]. Figure 1 shows the axial electric field for the varying geometries, and Figure 2 shows the geometry of the rf photoinjector for 1.45 cells.

### *Genetic Optimizer*

The two objectives are a small transverse emittance and a short bunch length. The variables for the simulation are the

\* Work Supported by DOE/SU Contract DE-AC02-76-SF00515, US NSF Award PHY-1549132, the Center for Bright Beams, and DOE SCGSR Fellowship. Travel to IPAC'17 supported by the Div. of Phys. of the US NSF (Accel. Sci. Prog.) and the Div. of Beam Phys. of the APS

<sup>†</sup> acahill@physics.ucla.edu

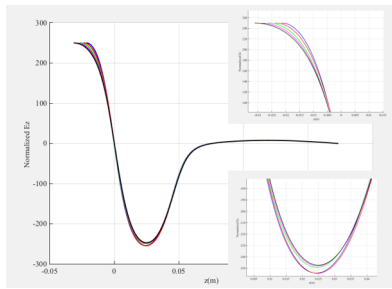


Figure 1: Axial electric fields for a 1.4, 1.45, 1.5, 1.55, and 1.6 cell rf photoinjector, scaled to 240 MV/m on the cathode.

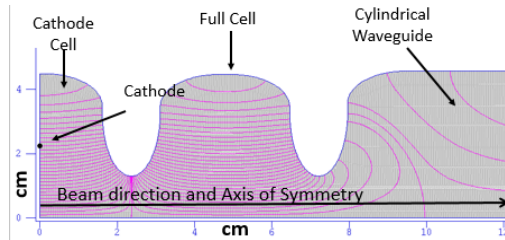


Figure 2: The geometry for a 1.45 cell photoinjector

laser spot size and its temporal length, the initial rf phase relative to the laser, the solenoid position and maximum field, and the linac position and its rf phase. Figure 3 shows a diagram of the simulation setup. The initial thermal emittance used for these simulations is 0.56 mm-mrad per rms mm of the laser spot size. The initial particle distributions are uniformly filled ellipsoids. For the smallest emittances, it corresponds to the cigar shape regime (small transverse cross-section and elongated pulse) [13]. For the short electron bunch it corresponds to the pancake regime.

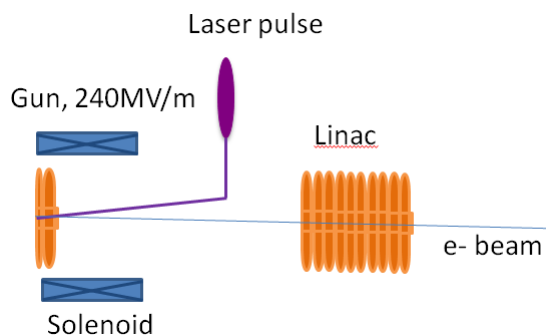


Figure 3: Setup of the Astra simulation. Initially, a laser is sent into the cavity to promote electrons. The electrons are accelerated by the photogun and focused by a solenoid. They reach an accelerating structure after propagating through in a drift section of adjustable length.

The optimizer routine begins by generating a random set of initial points for the variables stated above. These initial points are used to propagate a beam through the simulated rf photoinjector, using Astra [14] to calculate the emittance and bunch length. The initial population is sorted by dominance, where any non dominated solution, a solution where

no others have an improvement in either objective without degrading the other objective, is given rank 1. Solutions that are dominated by only those in the first group are given rank 2 and so on [9]. Solutions are chosen, by minimizing dominance rank and maximizing the distance between solution points, to be the parents to the next generation of solutions. This next generation is then created by crossover and mutation operators and simulated using Astra. The process continues until a diverse set of non-dominated solutions is found, giving the pareto plot that shows the trade-off between horizontal emittance and rms bunch length.

## RESULTS

The simulation was run for different bunch charges: 10 pC, 100 pC, and 1 nC. We focused on the two extremes of cathode cell length, simulating 1.4 and 1.6 cell rf photogun geometries.

### 10 pC

The results for a small bunch charge show horizontal emittance of 10 nm · rad, and a peak brightness of 250 nC/(mm · mrad)<sup>2</sup>/mm. As can be seen in Fig. 3, the difference between a 1.4 and 1.6 cell geometry is small but noticeable in emittance, and leads to a 20% increase in brightness for the 1.4 cell case relative to the 1.6 cell case. Figure 4 shows the pareto plot and brightness for 10 pC.

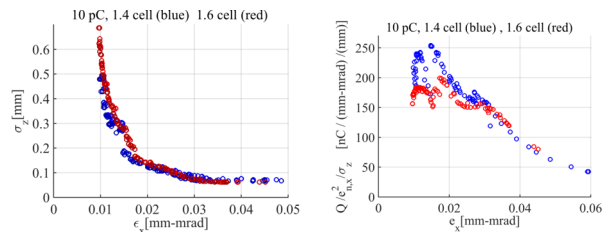


Figure 4: Left) The optimal horizontal emittance and rms bunch length are plotted for 10 pC for 1.4 and 1.6 cell geometries. Right) Brightness vs transverse emittance. The shorter cathode cell leads to 20% larger beam brightness

### 100 pC

For 100 pC there is very little difference in the optimal horizontal emittance and rms bunch length for two different cell lengths as can be seen in Fig. 5. The maximum brightness is 80 nC/(mm · mrad)<sup>2</sup>/mm, and the horizontal emittance reaches 45 nm · rad, which is smaller by 50% than the emittance in an optimized photoinjector with the S-Band gun operated at 120 MV/m. [4].

### 1 nC

In the high charge case the brightness is larger when the cathode cell is longer, the 1.6 cell geometry has a peak beam brightness of 25 nC/(mm · mrad)<sup>2</sup>/mm against 15 nC/(mm · mrad)<sup>2</sup>/mm for the 1.4 cell geometry (see Fig. 6b). The transverse emittance for the longer geometry is 250 nm · rad. Figure 6 shows the pareto plot and brightness for 1 nC.

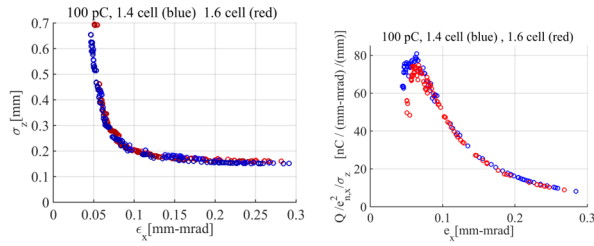


Figure 5: Left) The optimal horizontal emittance and rms bunch length are plotted for 100 pC for 1.4 and 1.6 cell geometries. There is minimal difference between the two cases. Right) Beam brightness vs transverse emittance.

In these simulations, we noticed two sets of results: (1) where the linac was close to the rf gun exit at 0.6 m from the cathode, and (2) where the linac was 1.9 m downstream, further from the rf gun. When the linac was close, the brightness was optimized, while when the linac was far, the electron beam reached very short bunch lengths, which is shown in Fig. 6a. For our very high gradient, 240 MV/m, optimizing for brightness, it is important to have the linac close to minimize the time of space-charge expansion, also true in the two lower charge cases. However, if the linac is further from the rf gun for the high charge case, short bunch lengths can be created using velocity bunching while the electrons are at a relatively low energy.

This is different than results found in [4], where the linac is placed further away, near 2m for low charges. However, results presented in [4] were for at 120 MV/m, which may explain the difference.

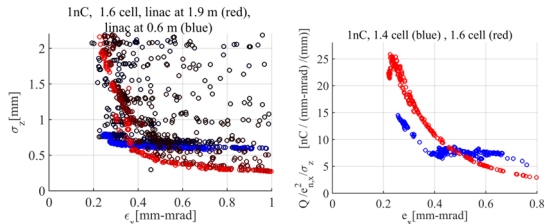


Figure 6: Left) Optimal horizontal emittance and rms bunch length are plotted for a 1.6 cell geometry for two positions of the linac, close to the gun at 0.6 m and far from the gun at 1.9 m downstream. Right) The brightness versus transverse emittance. Beam brightness of the longer cathode cell is larger.

### Time of Flight

Figure 7 shows the time of flight and energy for the rf gun phase at the launch of the electron beam. The 1.4 cell geometry operates between -10 and -5 degrees, depending on charge and bunch length goals, where this injection phase will depend on the bunch charge. The 1.6 geometry operates between +5 and +10 degrees depending on goals. These phases are close to a phase of zero, where the variation in arrival time to change in phase is 7.9 fs/deg for the 1.4 cell gun and 65.6 fs/deg in the 1.6 cell geometry. This makes

the 1.4 cell gun much more attractive for requirements on phase for arrival time stability. In addition, the arrival time will vary with a change in voltage, 10 fs per 0.1 % change in voltage on the cathode. We see that the shorter cathode cell is significantly more stable for arrival time.

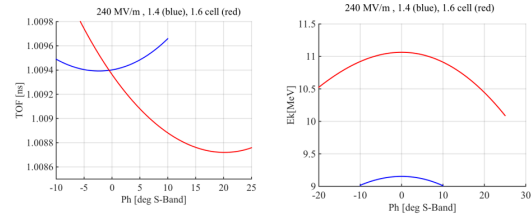


Figure 7: Left) time of flight vs rf gun phase, where 0 deg is the maximum energy. Right) Energy at gun exit vs gun phase.

### Differences Between 1.4 and 1.6 Cell RF Gun

Another difference between the 1.4 and 1.6 cell geometries is the beam energy at the gun exit, as shown in Fig. 7. Since the energy is larger in the 1.6 cell geometry, the solenoid requires a larger field, around 0.81 T, while the shorter 1.4 cell geometry requires 0.66 T. Decreasing the solenoid requirements make the 1.4 cell geometry advantageous in this respect.

In the 1.6 cell geometry, the electrons leave the gun at a phase where the defocusing kick is more linear [15]. This becomes important for a high charge bunch which is substantially elongated in time due to strong space charge forces. This is not as detrimental for low charge bunches which are short. This explains why the 1.6 cell gives smaller emittances than the 1.4 cell at 1 nC.

## CONCLUSION

In this paper we used a multi-objective optimizer on top of the ASTRA code to search for optimal solutions for competing goals of small emittance and small bunch length in a system comprising an S-band rf gun run at 240 MV/m on cathode and a linac, and this for a variety of charges. As the bunch charge decreases the beam brightness increases, where the maximum brightness we achieved is  $250 \text{ nC} / (\text{mm} \cdot \text{mrad})^2 / \text{mm}$  at 10 pC. The length of the cathode cell is an important choice and depends on the bunch charge. For small bunch charge, of 10 pC, the shorter 1.4 cell geometry outperformed the 1.6 cell geometry. Whereas for a high bunch charge the opposite was true. The crossover is around 100 pC, where the 1.4 and 1.6 cell geometries gave similar results. As well as the choice of cathode cell length, the position of the booster linac needs to be considered, where placing the linac closer to the gun optimizes the injector system for brightness, while placing the linac further away can create shorter electron bunches. Finally, the shorter cathode cell will have better arrival stability, and lower field solenoid. In the future, we plan to extend this study to both C-band and X-band frequencies.

## REFERENCES

- [1] D.T. Palmer et al. “Emittance Studies of the BNL/SLAC/UCLA 1.6 cell Photocathode RF Gun.” In: Proc. of PAC97, 1997, pp. 2687–2689.
- [2] P. Emma et al. “First Lasing and Operation of an Angstrom-Wavelength Free-Electron Laser.” In: Nature Photonics 4 (2010).
- [3] D.H. Dowell et al. “Commissioning Results of the LCLS Injector.” In: Proc. of FEL07, 2007, pp. 276–283.
- [4] H. Qian, D. Filippetto, and F. Sannibale. “S-Band Photoinjector Investigations by Multi-Objective Genetic Optimizer.” In: Proc. of IPAC16, 2016, pp. 3979–3982.
- [5] J. B. Rosenzweig et al. “Next Generation High Brightness Electron Beams From Ultra- High Field Cryogenic Radiofrequency Photocathode Sources.” Preprint on Arxiv:1603.01657.
- [6] V. A. Dolgashev et al. “Preliminary Results of High Power Tests of Normal Conducting Cryo Cavity.” In: Presented at HG2015 Shanghai, China (2015).
- [7] C.F. Papadopoulos et al. “RF Injector Beam Dynamic Optimization for LCLS-II.” In: Proc. of IPAC14, 2014, pp. 1974–1976.
- [8] J. Qiang and C. Mitchell. “An Adaptive Unified Differential Evolution Algorithm for Global Optimization.” In: LBNL Report LBNL-6853E (2015).
- [9] K. Deb, A. Pratap, S. Agarwal, and T. Meyarivan. “A Fast and Elitist Multiobjective Genetic Algorithm: NSGA-II.” In: IEEE Transactions of Evol. Comp. 6 (2 2002).
- [10] A. Hofler et al. “Innovative Applications of Genetic Algorithms to Problems in Accelerator Physics.” In: PRST-AB 16 (2013).
- [11] K. Halbach and R. F. Holsinger. “SUPERFISH - A Computer Program for Evaluation of RF Cavities with Cylindrical Symmetry.” In: Particle Accelerators 7 (1976).
- [12] A.D. Cahill, V.A. Dolgashev, and M. Dal Forno. “Automated Design for Standing Wave Electron Photoguns: TOPGUN RF Design.” In: Proc. of IPAC16, 2016, pp. 3999–4001.
- [13] D. Filippetto, P. Musumeci, M. Zolotarev, and G. Stupakov. “Maximum Current Density and Beam Brightness Achievable by Laser-Driven Electron Sources.” In: PRST-AB 17 (2014).
- [14] K. Floettmann. “Astra: A Space Charge Tracking Algorithm.” In: <http://www.desy.de/~mpyf10/>
- [15] Kwang-Je Kim. “RF and Space-Charge Driven RF Electron Guns.” In: NIM A 275 (1989).